



THE UNIVERSITY *of* EDINBURGH

Edinburgh Research Explorer

A study on the possible usefulness of detrended fluctuation analysis of the electroencephalogram background activity in Alzheimer's disease

Citation for published version:

Abasolo, D, Hornero, R, Escudero, J & Espino, P 2008, 'A study on the possible usefulness of detrended fluctuation analysis of the electroencephalogram background activity in Alzheimer's disease' IEEE Transactions on Biomedical Engineering, vol 55, no. 9, pp. 2171-2179., 10.1109/TBME.2008.923145

Digital Object Identifier (DOI):

[10.1109/TBME.2008.923145](https://doi.org/10.1109/TBME.2008.923145)

Link:

[Link to publication record in Edinburgh Research Explorer](#)

Document Version:

Author final version (often known as postprint)

Published In:

IEEE Transactions on Biomedical Engineering

General rights

Copyright for the publications made accessible via the Edinburgh Research Explorer is retained by the author(s) and / or other copyright owners and it is a condition of accessing these publications that users recognise and abide by the legal requirements associated with these rights.

Take down policy

The University of Edinburgh has made every reasonable effort to ensure that Edinburgh Research Explorer content complies with UK legislation. If you believe that the public display of this file breaches copyright please contact openaccess@ed.ac.uk providing details, and we will remove access to the work immediately and investigate your claim.



A study on the possible usefulness of detrended fluctuation analysis of the electroencephalogram background activity in Alzheimer's disease

Daniel Abásolo¹, *Member, IEEE*, Roberto Hornero¹, *Member, IEEE*, Javier Escudero¹,
Student Member, IEEE, and Pedro Espino²

¹E.T.S. Ingenieros de Telecomunicación, University of Valladolid, 47011, Valladolid,
Spain

²Hospital Clínico San Carlos, c/Profesor Martín Lagos s/n, 28040, Madrid, Spain

AUTHOR'S ADDRESS: Daniel Abásolo
Biomedical Engineering Group
E.T.S. Ingenieros de Telecomunicación
University of Valladolid
Camino del Cementerio s/n
47011, Valladolid
Spain
Phone: +34 983 423981
Fax: +34 983 423667
E-mail: daniel.abasolo@tel.uva.es

Manuscript received June 19, 2007; revised January 5, 2007. This work was supported by grant project VA108A06 from Consejería de Educación de la Junta de Castilla y León. *Asterisk indicates corresponding author.*

*D. Abásolo is with the Biomedical Engineering Group, Department of Signal Theory and Communications, E.T.S.I. de Telecomunicación, University of Valladolid, Camino del Cementerio s/n, 47011, Valladolid, Spain (e-mail: daniel.abasolo@tel.uva.es).

R. Hornero and J. Escudero are with the Biomedical Engineering Group, Department of Signal Theory and Communications, E.T.S.I. de Telecomunicación, University of Valladolid, Spain.

P. Espino is with the Biomedical Engineering Group and the Hospital Clínico San Carlos, Madrid, Spain.

Abstract—We studied the electroencephalogram (EEG) background activity of Alzheimer’s disease (AD) patients with Detrended Fluctuation Analysis (*DFA*). *DFA* provides an estimation of scaling information and long-range correlations in time series. We recorded the EEG in 11 AD patients and 11 age-matched controls. Our results showed two scaling regions in all subjects’ channels (for limited time scales from 0.01 s to 0.04 s and from 0.08 s to 0.43 s, respectively), with a clear bend when their corresponding slopes (α_1 and α_2) were different. No significant differences between groups were found with α_1 . However, α_2 values were significantly lower in control subjects at electrodes T5, T6, and O1 ($p < 0.01$, Student’s *t*-test). These findings suggest that the scaling behavior of the EEG is sensitive to AD. Although α_2 values allowed us to separate AD patients and controls, accuracies were lower than with spectral analysis. However, a forward stepwise linear discriminant analysis with a leave-one-out cross-validation procedure showed that the combined use of *DFA* and spectral analysis could improve the diagnostic accuracy of each individual technique. Thus, despite spectral analysis outperforms *DFA*, the combined use of both techniques may increase the insight into brain dysfunction in AD.

Index Terms—Alzheimer’s disease, Detrended fluctuation analysis, Electroencephalogram, Scaling behavior

I. INTRODUCTION

Alzheimer's disease (AD) is a primary degenerative dementia of unknown etiology that gradually destroys brain cells and represents the most prevalent form of dementia in western countries [1]. AD is characterized by progressive impairments in cognition and memory whose course lasts several years prior to the death of the patient [2]. Structural changes in AD are related to the accumulation of amyloid plaques between nerve cells in the brain and with the appearance of neurofibrillary tangles inside nerve cells, particularly in the hippocampus and the cerebral cortex [3]. These two abnormal microscopic structures cause neuronal damage or death, which is followed by a chemical imbalance. Both structural and chemical changes produce a progressive cell death and an overall shrinkage of brain tissue, which culminates in the progressive clinical symptoms of AD [3].

The clinical diagnosis of AD is made primarily on the basis of medical history studies, psychiatric evaluation and different memory, reasoning and mental status tests. Nevertheless, the diagnostic accuracy values in AD are under 90% and a definite diagnosis is only possible by necropsy [4]. Thus, new approaches are necessary to improve AD diagnosis.

The electroencephalogram (EEG) has been used in dementia diagnosis for several decades. There are several reasons why intensive research has been performed on the EEG in AD. One is that AD is a cortical dementia in which EEG abnormalities are more frequently shown. Moreover, coherence analysis of the EEG in AD allows non-invasive assessment of synaptic dysfunction [2]. Conventional spectral analysis shows that one of the hallmarks in AD is a shift of the EEG power spectrum to lower frequencies [2], although in the early stages of the disease the EEG may exhibit normal frequencies [5]. A decrease of coherence among cortical areas has also been reported

[2]. From another point of view, several studies have examined the non-linear dynamics of the EEG in AD (a detailed review can be found in [2]). In general, the EEG is less complex and more regular in AD patients than in controls [2], [6], [7]. Moreover, AD patients' EEGs show reduced functional connections when compared to elderly controls [8]. These changes are likely due to decreased non-linear cell-dynamics and/or non-linear couplings among cortical areas as well as linear couplings [8], [9]. EEG abnormalities in AD are thought to be associated with functional disconnections among cortical areas resulting from death of cortical neurons, axonal pathology, cholinergic deficits, etc. [2].

The complex nature of the electrical brain activity results in a high degree of spatial and temporal fluctuations in the EEG [10]. To understand the EEG activity in a better way, it is important to characterize its fluctuations over different time scales. Recent studies indicate that EEG oscillations in the human brain show long-range temporal correlations [10]–[12].

In the present study, the scaling behavior of the EEG in AD was examined with Detrended Fluctuation Analysis (*DFA*). *DFA* provides an estimation of scaling information and long-range correlations in time series, and is known for its robustness against non-stationarities [10], [13], [14]. The information provided by *DFA* might have potential implications for the classification of EEGs in subtypes [10]. According to a recent physiologically based model of EEG generation, the main EEG scaling features and deviations from them could be related to the underlying physiology of dendritic propagation [15], which might be affected in different neurophysiologic states. We wanted to test the hypothesis that long-range temporal correlations in AD patients' EEGs would be different from those of age-matched controls and to check if these differences could be useful to distinguish both groups. We also performed a spectral

analysis to compare *DFA* results with the slowing of the EEG usually found in AD [2], [5] and studied whether the combined use of both techniques could improve AD diagnosis.

II. MATERIAL AND METHODS

A. Subjects

Twenty-two subjects participated in this study. Informed consent was obtained from all control subjects and all caregivers of the demented patients. The study was approved by the local ethics committee.

Eleven patients (5 men and 6 women; age = 72.5 ± 8.3 years, mean \pm standard deviation SD) fulfilling the criteria of probable AD were recruited from the Alzheimer's Patients' Relatives Association of Valladolid and referred to the University Hospital of Valladolid (Spain), where EEGs were recorded. The diagnosis was made on the basis of exhaustive medical, physical, neurological, psychiatric and neuropsychological examinations. Mini-Mental State Examination (MMSE) was used to assess the cognitive function [16]. The mean MMSE score for the patients was 13.1 ± 5.9 (mean \pm SD), with five of them having a score of less than 12 points, indicating a severe degree of dementia. Two patients were receiving lorapezepam. Although with therapeutic doses benzodiazepines may enhance beta activity, no prominent rapid rhythms were observed in the visual examination of their EEGs. None of the other patients used medication that could be expected to influence the EEG.

The control group consisted of 11 age-matched, elderly control subjects without past or present neurological disorders (7 men and 4 women; age = 72.8 ± 6.1 years, mean \pm SD). The MMSE score value for all control subjects was 30.

B. EEG recording

EEGs were recorded from the 19 scalp loci of the international 10-20 system (electrodes F3, F4, F7, F8, Fp1, Fp2, T3, T4, T5, T6, C3, C4, P3, P4, O1, O2, Fz, Cz, and Pz) using a Profile Study Room 2.3.411 EEG equipment (Oxford Instruments). More than five minutes of data were recorded from each subject. The sample frequency was 256 Hz, with a 12-bit A-to-D precision. Recording sessions were conducted with the subjects in an awake but resting state with eyes closed and under vigilance control.

All EEGs were visually inspected by a specialist physician to check for eye movement and other artifacts and only EEG data free from electrooculographic and movement artifacts, and with minimal electromyographic (EMG) activity were selected to be studied with *DFA*. EEGs were then organized in 5 second artifact-free epochs (1280 points). An average number of 30.0 ± 12.5 artifact-free epochs (mean \pm SD) were selected from each electrode for each subject. Furthermore, prior to the *DFA* all recordings were digitally filtered with a band-pass filter with cut-off frequencies at 0.5 Hz and at 40 Hz in order to remove residual EMG activity.

C. Detrended Fluctuation Analysis (DFA)

Since its introduction, the *DFA* has been established as an important tool for the detection of long-range correlations and fluctuations in different time series. For instance, it has been applied to evaluate characteristics of data such as DNA sequences [13], long-time weather records [17], sea clutter radar datasets [18] or heart rate dynamics [19], [20].

DFA has been used to detect long-range correlations in scalp EEG [10]. It has also been used to study the differences between the scaling properties of sleep EEG in patients with apnea and control subjects, and to relate them to the brain activity in different sleep stages [21]. Furthermore, it has been shown that *DFA* can be used to successfully distinguish patients with acute ischemic stroke from control subjects [10].

Moreover, it has provided a mean to discriminate among levels of consciousness during general anesthesia; different indexes derived from the scaling behavior of the EEG have been proposed to characterize the patient's state [22]. *DFA* has also been applied to study the EEG in AD, which is characterized by diminished fluctuations in the level of synchronization [23]. Changes in the scaling properties of the EEG in AD have also been investigated with *DFA* [24].

Let the EEG time series be denoted by $\{x(t)\}$, where t is the discrete time ranging from 1 to N ($N = 1280$). To perform the *DFA* of the EEG time series:

1. We integrate the time series. If $\overline{x(t)}$ represents the average value of $x(t)$, the integrated series is

$$y(n) = \sum_{t=1}^n [\{x(t)\} - \overline{x(t)}] \quad n = 1, \dots, N. \quad (1)$$

2. We divide the entire time range into B equal windows, discarding any remainder, so that each window has $k = \text{int}(N/B)$ time points ($\text{int}(a)$ denotes the integer part of a). We have used window or box sizes between 3 and 128 points, as one-tenth of the signal length can be considered as the maximum box size when using a *DFA* [14].
3. Within each window b ($b = 1, \dots, B$), we perform a least-square fit of $\{y(n)\}$ by a straight line $y_b(n)$. That is the semi-local trend for the b th window.
4. We define $F_b^2(k)$ to be the variance of the fluctuation $\{y(n)\}$ from $y_b(n)$ in the b th window

$$F_b^2(k) = \frac{1}{k} \sum_{n=(b-1)k+1}^{bk} [\{y(n)\} - y_b(n)]^2. \quad (2)$$

It is a measure of the semi-locally detrended fluctuation in window b .

5. The square root of the average of $F_b^2(k)$ over all windows is the rms fluctuation from the semi-local trends in B windows, each of k time points

$$F(k) = \sqrt{\frac{1}{B} \sum_{b=1}^B F_b^2(k)}. \quad (3)$$

Since *DFA* considers only the fluctuations from the semi-local trends, it is insensitive to spurious correlations introduced by slowly varying external trends [10].

The study of the dependence of $F(k)$ on the window size k is the essence of *DFA*. If there is a power-law behavior ($F(k) \propto k^\alpha$), α is an indicator of the nature of the fluctuations in the EEG. This exponent is 0.5 for uncorrelated white noise [23]. If $\alpha < 0.5$, the correlations in the signal are anti-persistent (i.e. an increment is very likely to be followed by a decrement, and vice versa), while if $0.5 < \alpha$ the correlations in the signal are persistent (i.e., an increment is very likely to be followed by an increment, and vice versa) [14]. The exponents estimated by *DFA* lie between 0 and 2 [25].

D. Spectral analysis

The power spectral density for each signal was estimated as the Fourier transform of the autocorrelation function. The powers were integrated in the following frequency bands: delta (0.5–4 Hz), theta (4–8 Hz), alpha (8–13 Hz), and beta (13–30 Hz). The relative power for each frequency band was computed by dividing the integrated value by the total power in the whole filtered band.

E. Statistical analysis

Student's *t*-test was used to evaluate the statistical differences between the scaling exponents from AD patients and control subjects and between the relative

powers of both groups for each frequency band. Differences were considered statistically significant if the p value was lower than 0.01.

The ability to discriminate AD patients from control subjects at the electrodes where $p < 0.01$ was evaluated using Receiver Operating Characteristic (ROC) curves [26] with a leave-one-out cross-validation procedure. Moreover, a forward stepwise linear discriminant analysis (LDA) with a leave-one-out cross-validation scheme was performed to assess whether spectral analysis and *DFA* could provide complementary information to improve AD diagnosis.

III. RESULTS

We performed *DFA* for channels F3, F4, F7, F8, Fp1, Fp2, T3, T4, T5, T6, C3, C4, P3, P4, O1, and O2. We studied the fluctuations using window sizes between 3 and 128 samples (from 0.01 s to 0.5 s). Furthermore, we plotted the natural logarithm of $F(k)$ as a function of the natural logarithm of k . If the plot displays a linear scaling region with a certain scaling exponent, then there is a power-law behavior in the time series.

We found two scaling regions in the EEG with a clear bend when the two slopes in the two regions are distinctly different. These scaling properties were found in all channels for all subjects. Fig. 1 and Fig. 2 show $F(k)$ vs. k in a log-log plot for one EEG epoch from a control subject at electrode T5 and for one EEG epoch from an AD patient at electrode T5, respectively. In both cases, two very different slopes can be seen and a bend in the transition between them can be observed. We have denoted α_1 the scaling exponent of the first region and α_2 the exponent on the second one.

 Insert Figures I and II around here

To quantify the scaling exponents, we performed a linear fit in region I for $1 < \ln k < 2.3$ (from 0.01 s to 0.04 s) and in region II for $3 < \ln k < 4.5$ (from 0.08 s to 0.43 s). The limits for $\ln k$ were chosen after a visual inspection of the results showed that fitting this way correctly characterizes the slopes in the two regions. The results were averaged based on all the artifact-free 5 second epochs within the five-minute period of EEG recordings. The α_1 and α_2 values (mean \pm SD) for the AD patients and control subjects are summarized in Tables I and II, respectively. No significant differences were found between the α_1 values of both groups ($p > 0.01$). On the other hand, α_2 values were lower in control subjects than in AD patients, with significant differences at electrodes T5, T6, and O1 ($p < 0.01$).

The intersection of the slopes α_1 and α_2 provides a good approximation of the bend position. Thus, we used this feature to estimate the value of $\ln k$ for which the slope between both scaling regions changes. Table III summarizes the obtained bend values. The bend is limited to a narrow range in most subjects and most channels corresponding to window sizes between 10 and 25 points (time scales from 0.04 to 0.10 s). No significant differences were found between both groups.

 Insert Tables I, II and III around here

The relative power values in the delta (0.5–4 Hz), theta (4–8 Hz), alpha (8–13 Hz), and beta (13–30 Hz) frequency bands (mean \pm SD) are shown in Table IV. AD patients are characterized by a shift of the power spectrum to lower frequencies. In fact, our results show an increase of the delta and theta activities, with significant differences at O2 and at F3, F7, and O1, respectively. Moreover, the power decrease in the alpha and beta bands is also reflected. The average relative power in the alpha band is

significantly lower in the AD patients at T3 and T4, while in the beta band a significant power decrease is found at O1 and O2.

 Insert Table IV around here

We used ROC plots to evaluate the ability of α_2 and the relative power values to discriminate AD patients from control subjects at electrodes where significant differences were found. In addition, leave-one-out cross-validation was used to prevent problems like over-fitting and bias. We have performed a subject-based classification, where the models were trained using all available data except for data from one subject. The excluded set was then used to test the performance of the model. The procedure was repeated for all subjects to obtain a more reliable estimate of classification performance. This method allows a larger training set to be used while still calculating the test error based on unseen data. This is very beneficial in situations where there is a limited amount of data available. We have also performed an epoch-based classification. The models were trained using all available data except for data from one epoch, which was then used to test the performance. This was done to take into account the variability of the results among different epochs from the same electrode and the same subject. In both classification schemes, the optimum threshold was the cut-off point in which the highest accuracy (i.e., maximum number of subjects/epochs correctly classified) was obtained. Results are shown in Table V in terms of sensitivity (true positive rate), specificity (true negative rate) and accuracy. The accuracies obtained with α_2 in the subject-based classification are between 63.64% and 72.73%. On the other hand, those obtained with the relative power in different frequency bands show more variability, ranging between 50% (alpha band relative power at T3) and 86.36%

(theta band relative power at O1). The epoch-based classification shows a slight but not significant change in the accuracy of the classification with α_2 . Conversely, the changes in the accuracies with the relative power and the epoch-based classification are greater. This probably reflects that the variability in the relative power is larger than that of α_2 among the analyzed EEG epochs.

 Insert Table V around here

A forward stepwise LDA with a leave-one-out cross-validation procedure was performed to check whether the combined use of spectral analysis and *DFA* could improve the subjects and epochs classification. LDA is used to model the behavior of a dependent categorical variable on the basis of one or more predictor variables (independent variables). LDA attempts to find the linear combinations of the independent variables that best distinguish the categories of the dependent variable. When trying to model the dependent variable from a set of predictors, the stepwise method can be useful to automatically select the “best” variables to be used in the model. Results are summarized in Table VI. In the subject-based classification, only 3 spectral analysis parameters were selected (alpha band power at T4, theta band power at F7 and beta band power at O1) among the 11 that were available (relative powers and α_2 values at electrodes where $p < 0.01$). An accuracy of 95.45% was achieved, implying an increase of 9.09% with respect to the best individual results, obtained with theta band power at O1. On the other hand, the discriminant model included parameters both from spectral analysis and *DFA* in the epoch-based classification scheme. In this case, eight parameters were automatically selected (firstly theta band power at O1, followed by beta band power at O1, alpha band power at T4, theta band power at F7, beta band

power at O2, α_2 at O1, α_2 at T6, and theta band power at F3, respectively) and an accuracy of 94.04% was achieved. This fact implies an increase of 15.26% with respect to the best individual accuracy results, obtained with theta band power at O1.

 Insert Table VI around here

It has been reported that crossovers of *DFA* plots can be caused by trends [14]. We used closed-eyes resting state EEG, resulting in a significantly strong alpha band. Thus, we wanted to examine if this issue might be causing the bending phenomena. In order to do so, we created new time series from the original EEG recordings using a band-stop filter to eliminate the alpha band and, subsequently, we performed *DFA* of these EEG time series. Fig. 3 illustrates the typical behavior found in control subjects. It shows $F(k)$ vs. k in a log-log plot for the EEG epoch used in Fig.1 and the results from the *DFA* of the EEG with the alpha band filtered out. It can be seen that the bending occurs at a lower value of $\ln k$ and is less clear than in Fig. 1. In addition, the slope in the second scaling region is steeper than originally. On the other hand, Fig. 4 is representative of the AD patients' behavior. It shows $F(k)$ vs. k in a log-log plot for the EEG epoch used in Fig. 2 and the results from the *DFA* of the EEG without the alpha band. In this case, the differences between both representations are not that clear, probably due to the low alpha power in the original EEG epoch of the AD patient.

 Insert Figures 3 and 4 around here

IV. DISCUSSION AND CONCLUSIONS

We analyzed the EEG background activity of 11 AD patients and 11 control

subjects with *DFA*, a technique that provides an estimation of scaling information and long-range correlations in time series. We found two different scaling regions in the EEG that depend on the window size k . The first region corresponds to small window sizes (less than 0.04 s) and could be characterized by a scaling exponent α_1 , with average values over 1.7. The second one corresponds to larger window sizes (from 0.08 s to 0.43 s) and could be described with an exponent α_2 , with average values between 0.59 and 1.07. For a certain window size between 10 and 25 data points (from around 0.04 s to 0.10 s), there is a bend – limited to a narrow range in most epochs – that marks a change in the nature of the fluctuations of the EEG. These scaling properties were found in all channels for all subjects.

DFA is one of the most frequently used methods to estimate the key scaling exponent: the Hurst parameter H [25]. It has been used to analyze long-range correlations in a wide variety of signals, which include the EEG. For instance, changes in the EEG in sleep stages [21] and other physiological states [11], [12] have been studied with *DFA*. Moreover, it has also been useful to characterize EEG changes in AD [23], [24]. The scaling behavior of the EEG as a measure of the level of consciousness during general anesthesia has also been studied with *DFA* [22]. Not only scalp EEG has been analyzed with this technique, as intracranial EEG *DFA* has shown that long-range correlations are also present in the hippocampus of epileptic patients [27], [28].

Most of these studies report one scaling region in the scalp EEG instead of two. However, due to the different range of window sizes inspected, comparisons with our study are not straightforward. In addition, in some studies long-range temporal correlations are obtained analyzing time series derived but different from the EEG, like the amplitude dynamics of alpha and beta oscillations [11], [12], the mean level of synchronization [23] or the “energy” of the signal obtained from the Cz electrode [29].

The scaling range in those studies was quite diverse (for instance, from 0.04 s to 5 s in [29] and from 5 s to 80 s in [11]). On the other hand, the results from [10] and [24] are in agreement with our study, in the sense that two scaling regions with a clear bend between them were found in the EEG. These studies also show that information provided by *DFA* has potential implications for the classification of EEGs in subtypes. Furthermore, in [10] the first region ranges from 0.01 s to 0.04 s, thus being similar to our region I, while the second one goes from 0.13 s to 1.25 s. Hence, the bending occurs at time scales similar to those reported here. Nevertheless, it must be noted that these results were obtained without integrating the EEG time series. Other study shows a breakpoint between scaling regions at around 0.1 s [24], something that is again consistent with our results. However, given the fact that the first scaling region is so short, the possible usefulness of the α_1 exponents is really limited. Two temporal scaling regimes in locally detrended human EEG fluctuation have also been reported in [15], where a model of EEG generation, which has been found to yield excellent agreement with observations of EEG spectra [30], evoked potentials [31] and normal arousal states and epileptic seizures [32], was used. The breakpoint between scaling regions was between 0.02 s and 0.1 s. Nevertheless, our results do not agree with the two scaling regions reported in [22], with time scales between 0.07 s and 0.16 s in the first one and from 1.58 s and 6 s (or 1.67 s and 7.5 s, depending on the epoch length) in the second one. However, it must be noted that the time scales from our region I were not analyzed in that study and the first region corresponds partially to our region II. Moreover, the scaling exponents in the awake state for time scales between 0.07 s and 0.16 s are similar to those obtained from the frontal electrodes in our study. In addition, the second scaling region in [22] is characterized by very low exponents. This might be showing that, as k increases, $F(k)$ would become a constant and the asymptotic slope would

become zero [10].

From the view of many body systems, long-range temporal correlations in the EEG should originate from the strong interactions of the neural cells. It is logical to assume that AD would weaken or even block the interactions. Therefore, one may expect that the temporal scaling behavior of the EEG would be sensitive to the individuals with or without AD [24]. This is reflected by the exponents obtained in the second scaling region and corroborates previously reported results [24] for time scales beginning at about 0.25 s. It is worth mentioning that the scaling exponents reported in [24] are lower than in our study.

The computation of the distinct slopes in each plot allowed us to determine the location of their intercept, which gives a good approximation to the position of the bend in the whole plot. Since scaling behavior means that the examined system has no intrinsic scale, scale non-invariance at the intercept implies that it is related to a characteristic time scale in the data [10]. It has been suggested that the time scale of the bend can be associated with a sine wave with frequency f calculated as the sampling rate divided by the window size of the intercept [10], which in our case lies between 0.04 s and 0.10 s, approximately. Thus, the bends would correspond to frequencies between 10 and 25 Hz and would have physiological meaning. However, this interpretation of the breakpoint in scaling behavior has been recently questioned using an EEG model [15]. This model predicts the power spectrum from quantities such as corticothalamic connectivities, synaptic strengths, dendritic time constants, neural conduction speeds, axonal ranges, and the effects of the EMG artifact [30]–[32]. Moreover, it explains the fluctuations in terms of the underlying power spectrum filtering implied by the detrending process [15]. It could be hypothesized that the significant differences between the α_2 values in AD patients and control subjects' EEGs might be due to brain

alterations in AD related to the model parameters. However, a suitable model to explain the impact of AD in the EEG considering the parameters of the aforementioned one has yet to be developed. Furthermore, the model suggests that the main breakpoint in the scaling is related primarily to dendritic filtering, rather than to alpha or beta band frequencies [15]. Nevertheless, our analysis of the EEG epochs with the alpha band filtered out shows that the bending and these frequencies are indeed related to a certain extent. Thus, it seems that one cannot rule out the influence of the alpha band in the bending phenomenon. However, despite the relevant differences found between the alpha relative power from AD patients and control subjects in the original EEG epochs, *DFA* did not reflect significant differences between the bend values of both groups. This leads us to think that a combination of different effects might be responsible for these bending phenomena.

One issue that also influences the temporal scaling regimes in the EEG is EMG activity [15]. Although all analyzed EEGs had minimal EMG activity and were filtered prior to *DFA* to remove residual EMG activity, jaw and facial muscles can yield significant contribution unless the subjects succeed to relax them [15]. These contributions vary with respect to the electrode, with minimal activity near the crown of the head (Cz electrode). In the presence of significant EMG activity, larger exponents should be found near the crown of the head than at electrodes near ear level, for window sizes in the tens of milliseconds [15]. Although the scaling exponents at P3 and P4 (close to Cz) are, in general, slightly higher than at other electrodes in region I (from 0.01 s to 0.04 s), the differences are small, suggesting that this effect is insignificant in our data.

No significant differences were found between AD patients and control subjects' scaling exponents at region I. However, α_2 values were significantly lower in control

subjects at T5, T6, and O1. We evaluated the possible usefulness of α_2 in AD diagnosis with ROC plots and a leave-one-out cross-validation procedure, obtaining accuracies around 70%. These values were lower than accuracies obtained with spectral analysis. Moreover, our results using *DFA* and spectral analysis are not completely consistent. This might be due to the fact that EEG signals are only approximately fractals in a very limited time scale range. Experimental data are always finite, and therefore may not conform to the ideal definition of fractal processes with long-range correlations [25]. Given the fact that *DFA* showed significant differences between groups at some electrodes where spectral analysis failed to separate AD patients from controls and vice versa, we inspected whether both techniques may contain complementary information that could improve AD diagnostic accuracy. In order to do so, a forward stepwise LDA with a leave-one-out cross-validation procedure was performed. In the subject-based classification three spectral analysis parameters were selected. With this model, an accuracy of 95.45% was achieved, improving by 9.09% the highest accuracy obtained with a single parameter (theta band power at O1). However, the results of this subject-based classification model should be taken with caution due to the reduced sample size, since 11 parameters were used to classify 22 subjects. On the other hand, the amount of data available for analysis is much larger in the epoch-based classification, since more than 600 epochs were processed. In this case, the discriminant model included parameters both from spectral analysis and *DFA*. An accuracy of 94.04% was achieved, representing an increase of 15.26% with respect to the highest accuracy obtained with a single parameter (theta band power at O1). This implies that the combination of *DFA* and spectral analysis may provide a more reliable model to detect AD from EEG epochs than that obtained using single parameters. It is noteworthy that these combined models correctly detected some subjects/epochs misclassified by one or more single parameters.

We have previously analyzed the same dataset with non-linear techniques, obtaining accuracies – without a leave-one-out cross-validation procedure – between 72.72% and 81.81% with sample entropy [7] and Lempel-Ziv's complexity [33]. However, comparison of results is not easy, as *DFA* inspects signal properties in different time scales. Recently, multiscale entropy (*MSE*) has been introduced to quantify signal complexity considering several time scales [34]. The analysis of our database with *MSE* showed important differences between AD patients and control subjects on the larger time scales, with significant differences at 10 electrodes ($p < 0.01$) [35]. The classification accuracies using the slope of the *MSE* profiles for those scales were between 77.27% and 90.91%. However, the analyzed time scales were not the same as in this study and a leave-one-out cross-validation procedure was not used. A related but much easier to compute multiscale measure, the scale-dependent Lyapunov exponent, has been recently proposed [36]. Due to its ability to characterize different types of motions, its performance in AD patients' EEG analysis should be checked.

Some limitations of our study merit consideration. First of all, our results from *DFA* and spectral analysis are not completely consistent. This could mean that EEG signals are only approximately fractals in a very limited time scale range. In fact, the fractal scaling behavior identified from the EEG in our study is only valid within very limited time scale ranges (from 0.01 s to 0.04 s and from 0.08 s to 0.43 s). The second scaling region may correspond to a larger one, as shown in other EEG studies, but we are limited by the available epoch length. Although our results show that the combined use of spectral analysis and *DFA* could improve AD diagnosis accuracy, further studies with a larger sample size are required to prove the usefulness of our methodology. Moreover, as AD diagnosis is only definite after necropsy, the sample may not fully represent this disease. Finally, the scaling properties of the EEG should be studied in

depression or other dementias to verify if the reported changes are specific to AD.

In summary, *DFA* shows two scaling regions in the EEG with a breakpoint between them that might have biological significance. Although scaling exponents for large window sizes allowed us to separate AD patients and control subjects, accuracies were lower than using spectral analysis. However, due to the approximately fractal nature of the EEG, the combined use of *DFA* and spectral analysis improved the AD diagnostic accuracy of each individual technique. *DFA* of the EEG in AD patients may increase the insight into brain dysfunction in this dementia and complement the classification based on spectral techniques.

ACKNOWLEDGMENT

The authors are thankful for the useful feedback of the Associate Editor and the Reviewers on the original manuscript.

BIOGRAPHY

Daniel Abásolo (M'04) was born in Valladolid, Spain, in 1976. He received the engineer degree in telecommunication engineering and the Ph.D. degree from the University of Valladolid, Valladolid, Spain, in 2001 and 2006, respectively.

He is currently Senior Lecturer in the Department of Signal Theory and Communications at the University of Valladolid. His main research interest is nonlinear biomedical signal processing.

Dr. Abásolo is a member of the Biomedical Engineering Group and the Spanish Biomedical Engineering Society (SEIB).

Roberto Hornero (M'04) was born in Plasencia, Spain, in 1972. He received his degree in Telecommunication Engineering and Ph.D. from the University of Valladolid, Spain, in 1995 and 1998, respectively.

He is currently Associate Professor (“Profesor Titular”) in the Department of Signal Theory and Communications at the University of Valladolid. His main research interest is nonlinear analysis of biomedical signals to help physicians in the clinical diagnosis. He founded the Biomedical Engineering Group in 2004. The research interests of this group are connected with the field of nonlinear dynamics, chaotic theory, and wavelet transform with applications in biomedical signal and image processing.

Dr. Hornero is a member of the Spanish Biomedical Engineering Society (SEIB).

Javier Escudero (S'07) was born in Valladolid, Spain, in 1982. He received the degree in telecommunication engineering from the University of Valladolid, Valladolid, Spain, in 2005. He is currently a scholarship holder in the Department of Signal Theory and

Communications at the University of Valladolid, where he is working toward the Ph.D. degree.

His main research interests are blind source separation techniques and nonlinear signal processing. He is a member of the Biomedical Engineering Group.

Mr. Escudero was awarded the Third Prize of the 2007 EMBS Student Paper Competition.

Pedro Espino received his degree in Medicine at the Complutense University of Madrid (Spain) in 1977. He specialized in Clinical Neurophysiology at the University Hospital of Madrid and obtained his Ph.D. at the University of Valladolid.

He currently works in the Clinical Neurophysiology Department of the Hospital Clínico San Carlos of Madrid. He is a member of the Biomedical Engineering Group, where he collaborates in the analysis of EEG and EMG signals.

TABLE AND FIGURE CAPTIONS

TABLE I Average values of the slope in the first scaling region

TABLE II Average values of the slope in the second scaling region. Significant differences are marked with an asterisk

TABLE III Average values of the estimated change of slope between the two scaling regions in the EEG

TABLE IV Relative power values (Mean \pm SD) in the delta (0.5–4 Hz), theta (4–8 Hz), alpha (8–13 Hz), and beta (13–30 Hz) frequency bands for AD patients and control subjects. Significant group differences are marked with an asterisk

TABLE V Sensitivity, specificity and accuracy values obtained with ROC curves and leave-one-out cross-validation

TABLE VI Sensitivity, specificity and accuracy values obtained with a forward stepwise LDA and leave-one-out cross-validation

Fig. 1. $F(k)$ vs. k in a log-log plot for one EEG epoch from electrode T5 of a control subject. The scaling exponents α_1 and α_2 are depicted with a solid line and their numerical values included.

Fig. 2. $F(k)$ vs. k in a log-log plot for one EEG epoch from electrode T5 of an AD patient. The scaling exponents α_1 and α_2 are depicted with a solid line and their numerical values included.

Fig. 3. $F(k)$ vs. k in a log-log plot for the EEG epoch from Fig. 1 before (marked with ‘*’) and after (marked with ‘◇’) filtering the alpha band out.

Fig. 4. $F(k)$ vs. k in a log-log plot for the EEG epoch from Fig. 2 before (marked with ‘*’) and after (marked with ‘◇’) filtering the alpha band out.

TABLE I
AVERAGE VALUES OF THE SLOPE IN THE FIRST SCALING REGION

Electrode	Control subjects (mean \pm SD)	AD patients (mean \pm SD)	<i>p</i> -value
F3	1.8305 \pm 0.0848	1.8495 \pm 0.0769	0.5890
F4	1.8207 \pm 0.0661	1.8541 \pm 0.0807	0.3013
F7	1.8171 \pm 0.0879	1.7805 \pm 0.1086	0.3946
F8	1.7965 \pm 0.0869	1.7911 \pm 0.1065	0.8990
Fp1	1.8034 \pm 0.0856	1.8147 \pm 0.0665	0.7332
Fp2	1.8064 \pm 0.0816	1.8205 \pm 0.0590	0.6459
T3	1.7763 \pm 0.1179	1.7470 \pm 0.1170	0.5646
T4	1.7701 \pm 0.0950	1.7287 \pm 0.1126	0.3631
T5	1.8445 \pm 0.1054	1.8618 \pm 0.0668	0.6504
T6	1.8366 \pm 0.1120	1.8666 \pm 0.0807	0.4792
C3	1.8265 \pm 0.0852	1.8522 \pm 0.0920	0.5037
C4	1.8364 \pm 0.0870	1.8367 \pm 0.1006	0.9952
P3	1.8744 \pm 0.0954	1.9196 \pm 0.0564	0.1908
P4	1.8844 \pm 0.1119	1.9255 \pm 0.0478	0.2761
O1	1.8255 \pm 0.1218	1.8594 \pm 0.0743	0.4399
O2	1.8162 \pm 0.1223	1.8672 \pm 0.0791	0.2593

TABLE II
 AVERAGE VALUES OF THE SLOPE IN THE SECOND SCALING REGION. SIGNIFICANT
 DIFFERENCES ARE MARKED WITH AN ASTERISK

Electrode	Control subjects (mean \pm SD)	AD patients (mean \pm SD)	<i>p</i> -value
F3	0.8755 \pm 0.1890	0.9590 \pm 0.1794	0.3005
F4	0.9202 \pm 0.1934	0.9458 \pm 0.1603	0.7386
F7	0.8605 \pm 0.1595	0.9820 \pm 0.1661	0.0954
F8	0.8976 \pm 0.1388	0.9710 \pm 0.1590	0.2618
Fp1	0.9317 \pm 0.1575	1.0662 \pm 0.2085	0.1032
Fp2	0.9618 \pm 0.1662	1.0640 \pm 0.1850	0.1879
T3	0.7180 \pm 0.1265	0.8792 \pm 0.2009	0.0357
T4	0.7323 \pm 0.1128	0.8812 \pm 0.2699	0.1068
T5*	0.6403 \pm 0.1689	0.9107 \pm 0.2328	0.0054
T6*	0.6559 \pm 0.1295	0.9009 \pm 0.2483	0.0088
C3	0.7336 \pm 0.2038	0.8551 \pm 0.1790	0.1530
C4	0.7192 \pm 0.1560	0.8280 \pm 0.1785	0.1438
P3	0.6520 \pm 0.2292	0.9000 \pm 0.2466	0.0240
P4	0.6077 \pm 0.2160	0.8660 \pm 0.2607	0.0199
O1*	0.5990 \pm 0.1757	0.8821 \pm 0.2469	0.0057
O2	0.6238 \pm 0.2076	0.8846 \pm 0.2570	0.0165

TABLE III
 AVERAGE VALUES OF THE ESTIMATED CHANGE OF SLOPE BETWEEN THE TWO SCALING
 REGIONS IN THE EEG

Electrode	Control subjects (mean \pm SD)	AD patients (mean \pm SD)	<i>p</i> -value
F3	2.3109 \pm 0.3625	2.4581 \pm 0.3581	0.3494
F4	2.2686 \pm 0.3006	2.4839 \pm 0.2932	0.1045
F7	2.3766 \pm 0.3346	2.3476 \pm 0.3777	0.8509
F8	2.2952 \pm 0.3276	2.3786 \pm 0.3548	0.5730
Fp1	2.2497 \pm 0.4068	2.2239 \pm 0.5443	0.9013
Fp2	2.2451 \pm 0.3361	2.3337 \pm 0.3038	0.5242
T3	2.4331 \pm 0.2458	2.3687 \pm 0.3278	0.6078
T4	2.4101 \pm 0.2772	2.3489 \pm 0.2643	0.6023
T5	2.5885 \pm 0.2278	2.6536 \pm 0.1638	0.4504
T6	2.5577 \pm 0.2793	2.6300 \pm 0.1282	0.4444
C3	2.4370 \pm 0.3280	2.5108 \pm 0.2410	0.5544
C4	2.4535 \pm 0.3477	2.5287 \pm 0.1681	0.5257
P3	2.5787 \pm 0.3125	2.6896 \pm 0.1360	0.2932
P4	2.5982 \pm 0.3197	2.6863 \pm 0.1081	0.3969
O1	2.5957 \pm 0.2354	2.6583 \pm 0.1331	0.4518
O2	2.5680 \pm 0.2758	2.6606 \pm 0.1302	0.3260

TABLE IV
RELATIVE POWER VALUES (MEAN \pm SD) IN THE DELTA (0.5–4 Hz), THETA (4–8 Hz),
ALPHA (8–13 Hz), AND BETA (13–30 Hz) FREQUENCY BANDS FOR AD PATIENTS AND
CONTROL SUBJECTS. SIGNIFICANT DIFFERENCES ARE MARKED WITH AN
ASTERISK

DELTA BAND (0.5-4 Hz)				THETA BAND (4-8 Hz)			
Electrode	Control subjects (mean \pm SD)	AD patients (mean \pm SD)	<i>p</i> -value	Electrode	Control subjects (mean \pm SD)	AD patients (mean \pm SD)	<i>p</i> -value
F3	0.7121 \pm 0.1069	0.7123 \pm 0.1402	0.9961	F3*	0.0741 \pm 0.0149	0.1255 \pm 0.0531	0.0058
F4	0.6097 \pm 0.1589	0.6730 \pm 0.1432	0.3377	F4	0.0854 \pm 0.0238	0.1339 \pm 0.0539	0.0129
F7	0.6387 \pm 0.1914	0.6505 \pm 0.1330	0.8679	F7*	0.0840 \pm 0.0223	0.1366 \pm 0.0527	0.0063
F8	0.5968 \pm 0.1599	0.6500 \pm 0.1350	0.4092	F8	0.0874 \pm 0.0270	0.1345 \pm 0.0586	0.0250
Fp1	0.6620 \pm 0.1543	0.7039 \pm 0.1562	0.5347	Fp1	0.0762 \pm 0.0132	0.1217 \pm 0.0563	0.0168
Fp2	0.6743 \pm 0.1658	0.7418 \pm 0.1349	0.3069	Fp2	0.0764 \pm 0.0195	0.1119 \pm 0.0545	0.0558
T3	0.4793 \pm 0.1576	0.5716 \pm 0.1865	0.2245	T3	0.0912 \pm 0.0464	0.1379 \pm 0.0628	0.0608
T4	0.4460 \pm 0.1344	0.5776 \pm 0.1647	0.0534	T4	0.0976 \pm 0.0400	0.1375 \pm 0.0629	0.0913
T5	0.5164 \pm 0.1457	0.6259 \pm 0.1236	0.0719	T5	0.1028 \pm 0.0608	0.1774 \pm 0.0636	0.0108
T6	0.4266 \pm 0.1756	0.6293 \pm 0.1940	0.0183	T6	0.1001 \pm 0.0446	0.1513 \pm 0.0653	0.0441
C3	0.6093 \pm 0.2021	0.6838 \pm 0.1641	0.3537	C3	0.0822 \pm 0.0354	0.1245 \pm 0.0638	0.0691
C4	0.5925 \pm 0.2021	0.7002 \pm 0.1776	0.1993	C4	0.0770 \pm 0.0302	0.1143 \pm 0.0601	0.0812
P3	0.4755 \pm 0.1968	0.6558 \pm 0.1853	0.0387	P3	0.1090 \pm 0.0858	0.1575 \pm 0.0786	0.1819
P4	0.4026 \pm 0.1976	0.6400 \pm 0.1960	0.0104	P4	0.0967 \pm 0.0499	0.1437 \pm 0.0573	0.0534
O1	0.4247 \pm 0.2029	0.6095 \pm 0.1411	0.0222	O1*	0.0877 \pm 0.0287	0.1651 \pm 0.0570	0.0007
O2*	0.4002 \pm 0.1789	0.6088 \pm 0.1490	0.0075	O2	0.0927 \pm 0.0530	0.1527 \pm 0.0473	0.0110

ALPHA BAND (8-13 Hz)				BETA BAND (13-30 Hz)			
Electrode	Control subjects (mean \pm SD)	AD patients (mean \pm SD)	<i>p</i> -value	Electrode	Control subjects (mean \pm SD)	AD patients (mean \pm SD)	<i>p</i> -value
F3	0.0937 \pm 0.0655	0.0736 \pm 0.0527	0.4360	F3	0.1048 \pm 0.0651	0.0776 \pm 0.0469	0.2739
F4	0.1238 \pm 0.0900	0.0839 \pm 0.0447	0.2029	F4	0.1587 \pm 0.0825	0.0956 \pm 0.0559	0.0484
F7	0.1267 \pm 0.0935	0.0755 \pm 0.0421	0.1134	F7	0.1267 \pm 0.0913	0.1028 \pm 0.0500	0.4552
F8	0.1162 \pm 0.0681	0.0750 \pm 0.0385	0.0957	F8	0.1643 \pm 0.0846	0.1083 \pm 0.0532	0.0778
Fp1	0.0964 \pm 0.0736	0.0681 \pm 0.0459	0.2911	Fp1	0.1375 \pm 0.0869	0.0895 \pm 0.0588	0.1449
Fp2	0.0976 \pm 0.0659	0.0608 \pm 0.0365	0.1208	Fp2	0.1272 \pm 0.0851	0.0727 \pm 0.0459	0.0762
T3*	0.1643 \pm 0.0965	0.0712 \pm 0.0377	0.0074	T3	0.2088 \pm 0.1006	0.1552 \pm 0.1127	0.2533
T4*	0.1599 \pm 0.0665	0.0724 \pm 0.0420	0.0014	T4	0.2351 \pm 0.1174	0.1538 \pm 0.0822	0.0746
T5	0.1929 \pm 0.1319	0.0946 \pm 0.0427	0.0290	T5	0.1591 \pm 0.0715	0.0871 \pm 0.0469	0.0112
T6	0.2222 \pm 0.1252	0.1115 \pm 0.0918	0.0282	T6	0.2089 \pm 0.1291	0.0906 \pm 0.0609	0.0124
C3	0.1285 \pm 0.0805	0.0804 \pm 0.0511	0.1098	C3	0.1606 \pm 0.1403	0.0960 \pm 0.0643	0.1801
C4	0.1228 \pm 0.0703	0.0736 \pm 0.0536	0.0801	C4	0.1839 \pm 0.1549	0.0968 \pm 0.0729	0.1071
P3	0.2212 \pm 0.1524	0.0995 \pm 0.0702	0.0259	P3	0.1720 \pm 0.1226	0.0782 \pm 0.0610	0.0344
P4	0.2952 \pm 0.2112	0.1284 \pm 0.1178	0.0331	P4	0.1800 \pm 0.1235	0.0799 \pm 0.0573	0.0242
O1	0.2652 \pm 0.2097	0.1195 \pm 0.0751	0.0422	O1*	0.1800 \pm 0.0878	0.0902 \pm 0.0410	0.0060
O2	0.2724 \pm 0.1929	0.1345 \pm 0.1040	0.0500	O2*	0.1866 \pm 0.0935	0.0881 \pm 0.0411	0.0045

TABLE V
SENSITIVITY, SPECIFICITY AND ACCURACY VALUES OBTAINED WITH ROC CURVES AND
LEAVE-ONE-OUT CROSS-VALIDATION

Method	Electrode	Sensitivity (%)	Specificity (%)	Accuracy (%)
α_2	T5 SB	54.55	81.82	68.18
	T5 EB	54.05	85.19	69.10
	T6 SB	72.73	72.73	72.73
	T6 EB	60.98	79.50	69.91
	O1 SB	54.55	72.73	63.64
	O1 EB	60.98	81.71	71.07
Delta band power	O2 SB	81.82	72.73	77.27
	O2 EB	68.82	70.73	69.76
Theta band power	F3 SB	63.64	90.91	77.27
	F3 EB	64.54	76.92	70.43
	F7 SB	63.64	72.73	68.18
	F7 EB	53.76	92.90	72.69
	O1 SB	90.91	81.82	86.36
	O1 EB	70.52	87.50	78.78
Alpha band power	T3 SB	54.55	45.46	50.00
	T3 EB	89.02	47.81	69.22
	T4 SB	63.64	63.64	63.64
	T4 EB	65.32	72.46	68.66
Beta band power	O1 SB	81.82	72.73	77.27
	O1 EB	68.79	72.56	70.62
	O2 SB	81.82	63.64	72.73
	O2 EB	76.77	72.26	74.55

SB: SUBJECT-BASED CLASSIFICATION

EB: EPOCH-BASED CLASSIFICATION

TABLE VI
SENSITIVITY, SPECIFICITY AND ACCURACY VALUES OBTAINED WITH A FORWARD
STEPWISE LDA AND LEAVE-ONE-OUT CROSS-VALIDATION

Method	Scheme	Sensitivity (%)	Specificity (%)	Accuracy (%)
LDA ¹	SB	90.91	100	95.45
LDA ²	EB	95.59	92.17	94.04

SB: SUBJECT-BASED CLASSIFICATION; EB: EPOCH-BASED CLASSIFICATION

¹ SELECTED PARAMETERS: ALPHA BAND POWER AT T4, THETA BAND POWER AT F7, AND BETA BAND POWER AT O1

² SELECTED PARAMETERS: THETA BAND POWER AT O1, BETA BAND POWER AT O1, ALPHA BAND POWER AT T4, THETA BAND POWER AT F7, BETA BAND POWER AT O2, α_2 AT O1, α_2 AT T6, AND THETA BAND POWER AT F3

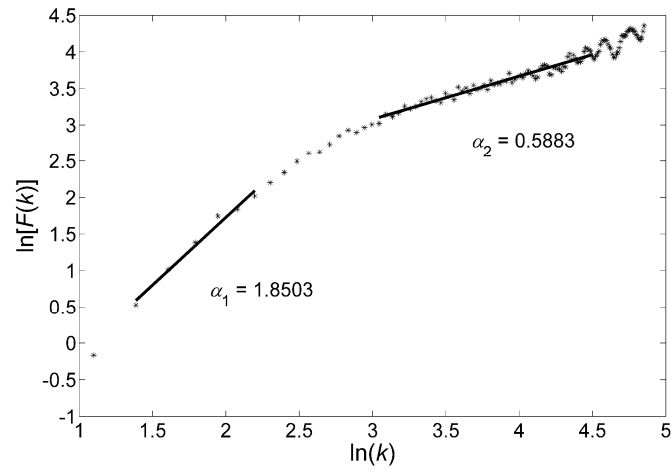


Fig. 1. $F(k)$ vs. k in a log-log plot for one EEG epoch from electrode T5 of a control subject. The scaling exponents α_1 and α_2 are depicted with a solid line and their numerical values included.

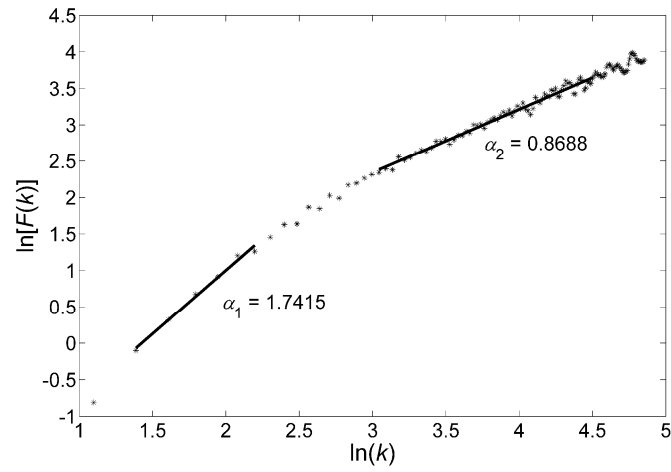


Fig. 2. $F(k)$ vs. k in a log-log plot for one EEG epoch from electrode T5 of an AD patient. The scaling exponents α_1 and α_2 are depicted with a solid line and their numerical values included.

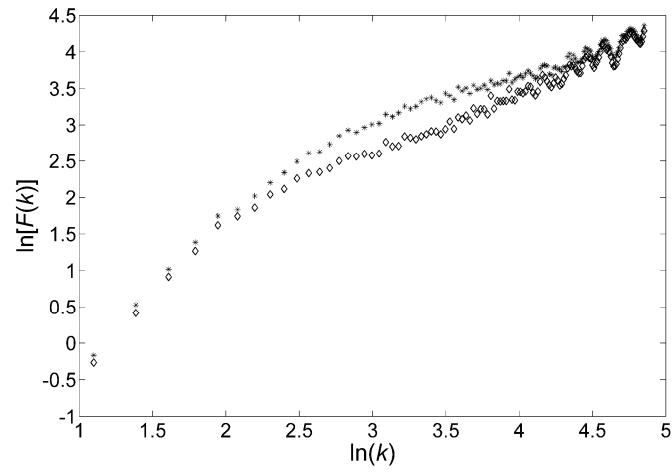


Fig. 3. $F(k)$ vs. k in a log-log plot for the EEG epoch from Fig. 1 before (marked with ‘*’) and after (marked with ‘◊’) filtering the alpha band out.

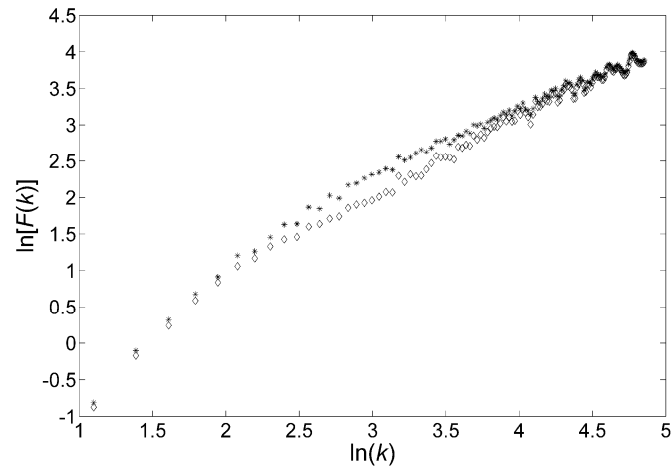


Fig. 4. $F(k)$ vs. k in a log-log plot for the EEG epoch from Fig. 2 before (marked with ‘*’) and after (marked with ‘ \diamond ’) filtering the alpha band out.

REFERENCES

- [1] T. D. Bird, "Alzheimer's disease and other primary dementias," in *Harrison's Principles of Internal Medicine*, E. Braunwald A. S. Fauci, D. L. Kasper, S. L. Hauser, D. L. Longo, and J. L. Jameson, Eds. New York: The McGraw-Hill Companies Inc, 2001, pp. 2391–2399.
- [2] J. Jeong, "EEG dynamics in patients with Alzheimer's disease," *Clin. Neurophysiol.*, vol. 115, pp. 1490–1505, Jul. 2004.
- [3] D. J. Selkoe, "Cell biology of the amyloid beta-protein precursor and the mechanism of Alzheimer's disease," *Annu. Rev. Cell. Biol.*, vol. 10, pp. 373–403, 1994.
- [4] M. Rossor, "Alzheimer's disease," in *Brain's Diseases of the Nervous System*, M. Donaghy, Ed. Oxford: Oxford University Press, 2001, pp. 750–754.
- [5] O. N. Markand, "Organic brain syndromes and dementias," in *Current Practice of Clinical Electroencephalography*, D. D. Daly and T. A. Pedley, Eds. New York, NY: Raven Press Ltd., 1990, pp. 401–423.
- [6] D. Abásolo, R. Hornero, P. Espino, J. Poza, C. I. Sánchez, and R. de la Rosa, "Analysis of regularity in the EEG background activity of Alzheimer's disease patients with Approximate Entropy," *Clin. Neurophysiol.*, vol. 116, pp. 1826–1834, Aug. 2005.
- [7] D. Abásolo, R. Hornero, P. Espino, D. Álvarez, and J. Poza, "Entropy analysis of the EEG background activity in Alzheimer's disease patients," *Physiol. Meas.*, vol. 27, pp. 241–253, Mar. 2006.
- [8] J. Jeong, J. C. Gore, and B. S. Peterson, "Mutual information analysis of the EEG in patients with Alzheimer's disease," *Clin. Neurophysiol.*, vol. 112, pp. 827–835, May 2001.

- [9] B. Jelles, J. H. van Birgelen, J. P. Slaets, R. E. Hekster, E. J. Jonkman, and C. J. Stam, "Decrease of non-linear structure in the EEG of Alzheimer patients compared to healthy controls," *Clin. Neurophysiol.*, vol. 110, pp. 1159–1167, Jul. 1999.
- [10] R. C. Hwa and T. C. Ferree, "Scaling properties of fluctuations in the human electroencephalogram," *Phys. Rev. E*, vol. 66, p. 021901, Aug. 2002.
- [11] V. V. Nikulin and T. Brismar, "Long-range temporal correlations in alpha and beta oscillations: effect of arousal level and test-retest reliability," *Clin. Neurophysiol.*, vol. 115, pp. 1896–1908, Aug. 2004.
- [12] V. V. Nikulin and T. Brismar, "Long-range temporal correlations in electroencephalographic oscillations: relation to topography, frequency band, age and gender," *Neuroscience*, vol. 130, pp. 549–558, 2005.
- [13] C.-K. Peng, S. V. Buldyrev, S. Havlin, M. Simons, H. E. Stanley, and A. L. Goldberger, "Mosaic organization of DNA nucleotides," *Phys. Rev. E*, vol. 49, pp. 1685–1689, Feb. 1994.
- [14] K. Hu, P. Ch. Ivanov, Z. Chen, P. Carpena, and H. E. Stanley, "Effect of trends on detrended fluctuation analysis," *Phys. Rev. E*, vol. 64, p. 011114, Jul. 2001.
- [15] P. A. Robinson, "Interpretation of scaling properties of electroencephalographic fluctuations via spectral analysis and underlying physiology," *Phys. Rev. E*, vol. 63, p. 032902, Mar. 2003.
- [16] M. F. Folstein, S. E. Folstein, and P. R. McHugh, "Mini-mental state. A practical method for grading the cognitive state of patients for the clinician," *J. Psychiatr. Res.*, vol. 12, pp. 189–198, Nov. 1975.
- [17] P. Talkner and R. O. Weber, "Power spectrum and detrended fluctuation analysis: Application to daily temperatures," *Phys. Rev. E*, vol. 62, pp. 150–160, Jul. 2000.

- [18] J. Hu, J. B. Gao, F. L. Posner, Y. Zheng, and W. W. Tung, "Target detection within sea clutter: a comparative study by fractal scaling analyses," *Fractals*, vol. 14, pp. 187–204, Sep. 2006.
- [19] P.-A. Absil, R. Sepulchre, A. Bilge, and P. Gérard, "Nonlinear analysis of cardiac rhythm fluctuations using DFA method," *Physica A*, vol. 272, pp. 235–244, Oct. 1999.
- [20] T. Penzel, J. W. Kantelhardt, L. Grote, J.-H. Peter, and A. Bunde, "Comparison of detrended fluctuation analysis and spectral analysis for heart rate variability in sleep and sleep apnea," *IEEE Trans. Biomed. Eng.*, vol. 50, pp. 1143–1151, Oct. 2003.
- [21] J.-M. Lee, D.-J. Kim, I.-Y. Kim, K. S. Park, and S. I. Kim, "Nonlinear-analysis of human sleep EEG using detrended fluctuation analysis," *Med. Eng. Phys.*, vol. 26, pp. 773–776, Nov. 2004.
- [22] M. Jospin, P. Caminal, E. W. Jensen, H. Litvan, M. Vallverdú, M. M. R. F. Struys, H. E. M. Vereecke, and D. T. Kaplan, "Detrended fluctuation analysis of EEG as a measure of depth of anesthesia," *IEEE Trans. Biomed. Eng.*, vol. 54, pp. 840–846, May 2007.
- [23] C. J. Stam, T. Montez, B. F. Jones, S. A. R. B. Rombouts, Y. van der Made, Y. A. L. Pijnenburg, and P. Scheltens, "Disturbed fluctuations of resting state EEG synchronization in Alzheimer's disease," *Clin. Neurophysiol.*, vol. 116, pp. 708–715, Mar. 2005.
- [24] C. P. Pan, B. Zheng, Y. Z. Wu, Y. Wang, and X. W. Tang, "Detrended fluctuation analysis of human brain electroencephalogram," *Phys. Lett. A*, vol. 329, pp. 130–135, Aug. 2004.

- [25] J. Gao, J. Hu, W.-W. Tung, Y. Cao, N. Sarshar, and V. P. Roychowdhury, "Assessment of long-range correlation in time series: How to avoid pitfalls," *Phys. Rev. E*, vol. 73, p. 016117, Jan. 2006.
- [26] M. H. Zweig and G. Campbell, "Receiver-Operating Characteristic (ROC) plots: a fundamental evaluation tool in clinical medicine," *Clin. Chem.*, vol. 39, pp. 561–577, Apr. 1993.
- [27] L. M. Parish, G. A. Worrell, S. D. Cranstoun, S. M. Stead, P. Pennell, and B. Litt, "Long-range temporal correlations in epileptogenic and non-epileptogenic human hippocampus," *Neuroscience*, vol. 125, pp. 1069–1076, 2004.
- [28] J. Bhattacharya, J. Edwards, A. N. Mamelak, and E. M. Schuman, "Long-range temporal correlations in the hippocampal-amygdala complex of humans," *Neuroscience*, vol. 131, pp. 547–555, 2005.
- [29] S. Leistedt, M. Dumont, J.-P. Lanquart, F. Jurysta, and P. Linkowski, "Characterization of the sleep EEG in acutely depressed men using detrended fluctuation analysis," *Clin. Neurophysiol.*, vol. 118, pp. 940–950, Apr. 2007.
- [30] P. A. Robinson, C. J. Rennie, J. J. Wright, H. Bahramali, E. Gordon, and D. L. Rowe, "Prediction of electroencephalographic spectra from neurophysiology," *Phys. Rev. E*, vol. 63, p. 021903, Jan. 2001.
- [31] C. J. Rennie, P. A. Robinson, and J. J. Wright, "Unified neurophysical model of EEG spectra and evoked potentials," *Biol. Cybern.*, vol. 86, pp. 457–471, Jun. 2002.
- [32] P. A. Robinson, C. J. Rennie, and D. L. Rowe, "Dynamics of large-scale brain activity in normal arousal states and epileptic seizures," *Phys. Rev. E*, vol. 65, p. 041924, Apr. 2002.

- [33] D. Abásolo, R. Hornero, C. Gómez, M. García, and M. López, “Analysis of EEG background activity in Alzheimer’s disease patients with Lempel-Ziv complexity and Central Tendency Measure,” *Med. Eng. Phys.*, vol. 28, pp. 315–322, May 2006.
- [34] M. Costa, A. L. Goldberger, and C.-K. Peng, “Multiscale entropy analysis of complex physiologic time series,” *Phys. Rev. Lett.*, vol. 89, p. 068102, Jul. 2002.
- [35] J. Escudero, D. Abásolo, R. Hornero, P. Espino, and M. López, “Analysis of electroencephalograms in Alzheimer’s disease patients with multiscale entropy,” *Physiol. Meas.*, vol. 27, pp. 1091–1106, Nov. 2006.
- [36] J. B. Gao, J. Hu, W. W. Tung, and Y. H. Cao, “Distinguishing chaos from noise by scale-dependent Lyapunov exponent,” *Phys. Rev. E*, vol. 74, p. 066204, Dec. 2006.